JACS
JOURNAL OF THE AMERICAN CHEMICAL SOCIETY
Communication
pubs.acs.org/JACS

Pt_5Gd as a Highly Active and Stable Catalyst for Oxygen Electroreduction

María Escudero-Escribano,[†] Arnau Verdaguer-Casadevall,[†] Paolo Malacrida,[†] Ulrik Grønbjerg,[†,‡] Brian P. Knudsen,[†] Anders K. Jepsen,[†] Jan Rossmeisl,[‡] Ifan E. L. Stephens,[†] and Ib Chorkendorff*[,†]

[†]Center for Individual Nanoparticle Functionality, Department of Physics, Building 312, Technical University of Denmark (DTU), DK-2800 Lyngby, Denmark

[‡]Center for Atomic-Scale Materials Design, Department of Physics, Building 307, Technical University of Denmark (DTU), DK-2800 Lyngby, Denmark

Supporting Information

ABSTRACT: The activity and stability of Pt_5Gd for the oxygen reduction reaction (ORR) have been studied, using a combination of electrochemical measurements, angle-resolved X-ray photoelectron spectroscopy (AR-XPS), and density functional theory calculations. Sputter-cleaned, polycrystalline Pt_5Gd shows a 5-fold increase in ORR activity, relative to pure Pt at 0.9 V, approaching the most active in the literature for catalysts prepared in this way. AR-XPS profiles after electrochemical measurements in 0.1 M $HClO_4$ show the formation of a thick Pt overlayer on the bulk Pt_5Gd, and the enhanced ORR activity can be explained by means of compressive strain effects. Furthermore, these novel bimetallic electrocatalysts are highly stable, which, in combination with their enhanced activity, makes them very promising for the development of new cathode catalysts for fuel cells.

Proton exchange membrane fuel cells (PEMFCs) are a potentially zero emission source of power, which are expected to play a key role in a future society based on sustainable energy. The main obstacle to the development of PEMFCs as a commercially competitive reality is the high overpotential required for the oxygen reduction reaction (ORR) to proceed at an adequate rate. Due to this fact, the ORR has been the most intensively studied fuel-cell reaction over the past decade.[1−7] The most active electrocatalysts known for the ORR are based upon Pt. However, high loadings of Pt are necessary at the cathode in order to achieve acceptable power densities.[1] In order to reduce the Pt loading, there is a need to develop novel catalysts with enhanced activity and long-term stability under operating conditions.[1,2]

The activity of Pt toward the ORR can be improved by slightly weakening its binding to the O-containing reaction intermediates, O, OH, and OOH. The optimal catalyst should have an OH binding energy ≈0.1 eV weaker than pure Pt.[4a] The most widely used approach to achieve this goal is to alloy Pt with other metals, such as Co, Ni, Fe, Cu, hence improving its ORR activity.[1,3−5,8] The more reactive solute metal, e.g. Co, Ni, Fe, Cu, will tend to dissolve in the acidic electrolyte of a PEMFC, leaving behind a Pt overlayer. Unless the catalyst has been pre-annealed,[3b,c,5b] this overlayer is typically several monolayers thick.[5a,8] On the acid leached catalysts, the weakening of the binding to OH occurs as a result of the compressive strain imposed onto the Pt-overlayer by the alloy bulk.

It is crucial to improve not only the fuel-cell cathode catalyst activity but also its durability. Alloys of Pt and late transition metals generally degrade by dealloying.[1b,4a,9] This involves the segregation of the solute metal to the surface[9a,c] and its subsequent dissolution. The susceptibility of Pt alloys with late transition metals, such as Fe, Co, Ni and Cu toward dealloying can be understood on the basis of their negligible heat of formation.

Recently, Pt_3Y was identified on the basis of density functional theory (DFT) calculations as being a catalyst that should be both active and stable for the ORR.[4a] Experiments confirmed that the catalyst exhibited the highest ORR activity ever measured for a polycrystalline surface.[1b,4] Alloys of Pt with early transition metals or rare earths, such as Y, Gd, or La, have exceptionally negative heats of formation;[1b,10,11] this should provide them with the kinetic stability to prevent dealloying under fuel cell reaction conditions, unlike alloys of Pt and late transition metals. This is because the kinetic barrier for solute metal diffusion through the alloy core and the thick Pt overlayer should be at least partially determined by the heat of formation. Moreover, despite their denomination, rare earths are more abundant, produced on a larger scale, and less expensive than Pt.[12] Very recent studies on Pt_xLa[1b,13] have demonstrated that these alloys present enhanced activity compared to pure Pt[1b] as well as high stability.[13] To the best of our knowledge, no other studies concerning the activity and/or the stability of Pt and rare earth metal alloys have been reported so far. Pt_5Gd is a very stable alloy, with a formation energy of −3.9 eV/formula unit,[11] similar to that of Pt_3Y[4a] and Pt_5La.[1b]

In this communication, we present, for the first time, experimental and theoretical studies concerning the activity and stability of Pt_5Gd for the ORR. The bulk, polycrystalline electrode was sputter cleaned in an ultrahigh-vacuum chamber, before being transferred to a rotating ring disk electrode (RRDE) assembly to conduct electrochemical measurements in 0.1 M $HClO_4$. Full experimental details can be found in the Supporting Information (SI).

Received: June 29, 2012
Published: September 21, 2012

 © 2012 American Chemical Society dx.doi.org/10.1021/ja306348d | J. Am. Chem. Soc. 2012, 134, 16476−16479

The activity of the catalyst toward the ORR was evaluated in an O_2-saturated 0.1 M $HClO_4$ solution, using cyclic voltammetry. Typical cyclic voltammograms (CVs) on sputter-cleaned Pt_5Gd and Pt polycrystalline electrodes in oxygen-saturated perchloric acid solutions are shown in Figure 1a. The ORR was measured once a stable CV was obtained in a

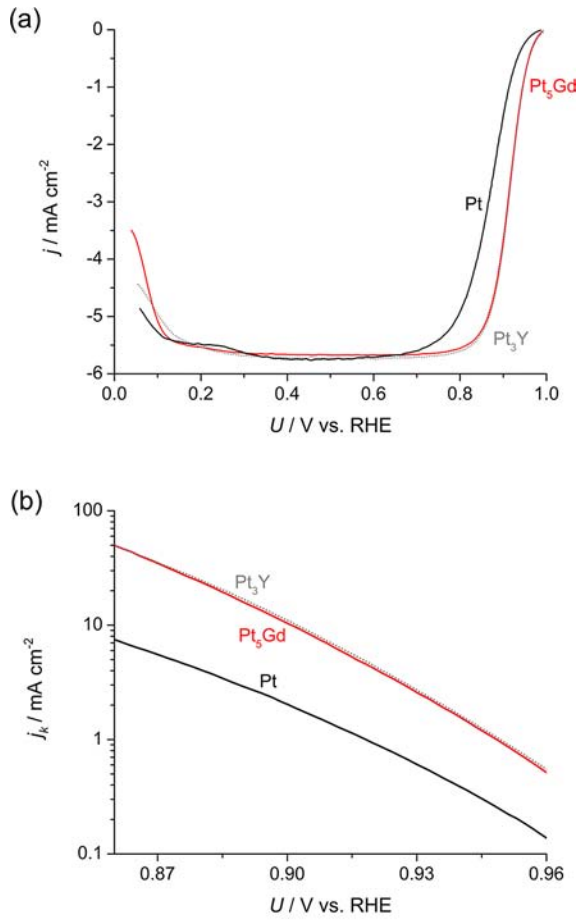

Figure 1. (a) RRDE polarization curves at 1600 rpm and 50 mV s^{-1} for the ORR on Pt_5Gd (red curve), Pt (black curve), and Pt_3Y (dotted gray curve) polycrystalline electrodes in O_2-saturated 0.1 M $HClO_4$. (b) Tafel plots showing the kinetic current density (j_k) of Pt_5Gd, Pt, and Pt_3Y as a function of the potential (U), based on data from (a).

nitrogen-saturated electrolyte (typically after ca. 100 cycles). On both electrodes, the onset for the ORR starts at ≈1 V, and the current increases exponentially with decreasing potential, characteristic of kinetic control. At more negative potentials, the current becomes increasingly controlled by mass transport, until it is completely transport limited, reaching the value of 5.7 mA cm^{-2}. We assume that the roughness factor was 1 cm^2/cm^2, as found for other Pt alloys tested for the ORR.[4] In the potential region of mixed kinetic transport, there is a considerable positive shift for Pt_5Gd, relative to Pt. This represents a substantial decrease in the overpotential for the alloy surface. Moreover, Figure 1 also shows that the ORR activity on Pt_5Gd is essentially the same as that of polycrystalline Pt_3Y (see gray dotted curve).[4] In the Tafel plot shown in Figure 1b, the kinetic current density, j_k, i.e., the current density in the absence of any mass-transfer effects, is represented as a function of the potential, U. Pt_5Gd exhibits a kinetic current density, at 0.90 V, $j_k = (10.4 \pm 0.2)$ mA cm^{-2}, which means that Pt_5Gd exhibits a 5-fold improvement over Pt. A similar enhancement was obtained on polycrystalline Pt_3Y (see gray dotted curve in Figure 1b).[4] Previous results on sputter-cleaned polycrystalline Pt_3M (M = Ni, Co, Fe) alloys by Stamenkovic et al.[3] showed up to 2-fold improvements in activity over pure Pt. However, our results show that Pt_5Gd and Pt_3Y[1b,4] present the highest activities for sputter-cleaned (Pt-skeleton)[3b] structures reported in the literature so far. According to these results, the ranking of ORR activity for the most active polycrystalline Pt alloys is in ascending order: Pt ≪ Pt_5La ≈ Pt_5Y < Pt_3Y ≈ Pt_5Gd.[1b]

In order to investigate the chemical composition of the active phase of the Pt_5Gd electrocatalyst, angle-resolved XPS (AR-XPS) experiments were carried out before and after the electrochemical measurements. After sputter cleaning the sample (before electrochemistry, see Figure 2a), the Pt to Gd

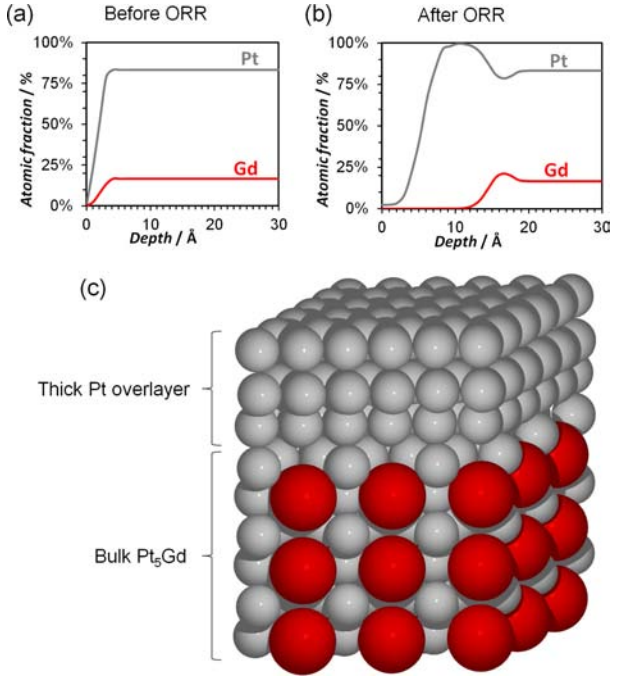

Figure 2. Nondestructive AR-XPS profiles of polycrystalline, sputter cleaned, Pt_5Gd before (a) and after (b) the ORR measurements. The adventitious C and O traces have been omitted for clarity; these are presumably accumulated during the transfer. The sputter cleaned sample exhibited a small submonolayer coverage of C and O, associated with the high sticking coefficient of any residual molecules on Gd, which is very reactive. (c) Schematic three-dimensional view of the structure shown in (b), consisting of a Pt (gray balls) overlayer, covering a bulk Pt_5Gd alloy (the large red balls are Gd atoms). In this case, the thickness of the Pt overlayer, at three monolayers, is arbitrary.

ratio was 5.0 ± 0.2, as estimated from three different measurements at 21° emission angle from the normal to the surface. At this angle, the surface sensitivity is lower, and the effects of possible differential sputtering are minimized. However, these do not seem to play an important role on the surface composition, as the Pt to Gd ratio does not change significantly with the emission angle (see Figure S8). Following the ORR experiments, the sample was transferred to the UHV chamber, and Pt to Gd ratio of 9.1 ± 0.9 was measured. This suggests that Gd is partially dissolved in the acidic electrolyte. Figure 2 shows the typical depth profiles of Pt_5Gd before (a) and after (b) ORR. Evidently a Pt overlayer with a thickness of

dx.doi.org/10.1021/ja306348d | J. Am. Chem. Soc. 2012, 134, 16476–16479

few Pt layers was formed. This is consistent with other acid leached Pt-skeleton alloys, including Pt_5La, Pt_5Y, and Pt_3Y.[1,4,14] Further investigations are underway to quantify the exact thickness of the Pt overlayer. Accordingly, the effect of alloying Pt is to impose strain onto the Pt overlayer. In the absence of Gd in the first three atomic layers, there would be no "ligand effect".[1b,15]

It must be noted that under the acidic and oxidizing operating conditions of a PEMFC, there would be a strong thermodynamic force toward the dissolution of Gd from Pt_5Gd: the standard dissolution potential, U_0, for Gd to Gd^{3+} is −2.40 V vs the normal hydrogen electrode (NHE)[16] (which means that the standard Gibbs free energy for the dissolution of Gd to Gd^{3+} is −7.20 eV), and the alloying energy of Pt_5Gd stabilizes each Gd atom by 3.9 eV.[11] Then, the standard Gibbs free energy for the dissolution of Gd to Gd^{3+} will be −3.30 eV, and the corresponding standard reduction potential is −1.10 V vs NHE. Hence, despite the stabilization of Gd atoms in the Pt_5Gd alloy by 3.9 eV, at 1 V vs NHE we are 2.1 V above the standard reduction potential, i.e., there is a driving force of −6.3 eV for the dissolution of each Gd atom. A similar driving force exists for the dissolution of other rare earths or early transition metals when alloyed with Pt, including Pt_3Y and Pt_5La, explaining why the solute metal will dissolve from these surfaces.[1b] However, this is inconsistent with reports that metallic La or Y could be present at the surface Pt_3La or Pt_3Y electrodes under ORR conditions.[13,17] Despite the thermodynamic driving force, the Pt overlayer provides kinetic stability against Gd dissolution from the alloy bulk.

DFT calculations were performed in order to understand the high ORR activity of Pt_5Gd. The Pt_5Gd structure was modeled following the same procedure as for Pt_5La,[1b] as a strained close-packed pure Pt overlayer. The surface strain was estimated on the basis that the Pt−Pt interatomic distance would be set by the bulk lattice parameter of Pt_5Gd, a = 0.522 nm (based on XRD measurements described in the SI). A schematic representation of the structure is shown in Figure 2c. This would lead to a Pt overlayer that is compressed by 6% relative to Pt(111). Our DFT calculations suggest that this strain would result in an excessive weakening of the OH binding energy, relative to Pt(111), of ≈0.3 eV. The compressive strain that would provide the optimal OH binding energy ≈0.1 eV weaker than Pt(111) would be 2%.[5a] On the basis of the DFT model, we would expect the perfect, defect-free surface to have a lower activity than pure Pt, in contradiction to our experiments.[7,18] However, we expect that on the experimentally tested phase of Pt_5Gd, the strain at the surface would be significantly lower than the 6% we estimate for a "perfect" overlayer on Pt_5Gd, due to relaxation effects.[5a,19]

In order to study the stability of polycrystalline Pt_5Gd electrodes in acidic solutions, we first performed an accelerated stability test (test I) consisting of continuous cycles from 0.6 to 1.0 V vs RHE in an oxygen-saturated 0.1 M $HClO_4$ electrolyte at 100 mV s^{-1} and 23 °C. The CVs in an O_2-saturated 0.1 M $HClO_4$ solution before and after 10 000 cycles (after around 20 h of experiments) between 0.6 and 1.0 V are shown in Figure S4. Figure 3a shows the Tafel plots for the ORR on Pt_5Gd before (red curve) and after (orange dotted curve) 10 000 cycles in the conditions described above. Interestingly, these results show that the percentage of activity loss after 10 000 cycles is 14%, most of this loss occurring in the first 2000 cycles. For comparison, when subject to the same treatment, polycrystalline Pt loses 5% of its initial activity after 10 000

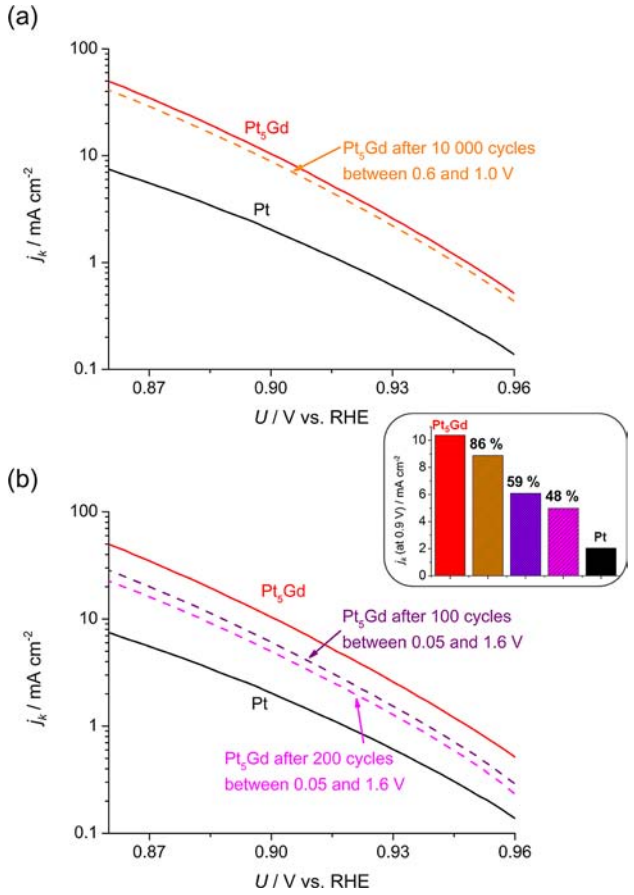

Figure 3. Tafel plots showing the stability of Pt_5Gd after: (a) 10 000 cycles between 0.6 and 1.0 V vs RHE at 100 mV s^{-1} (test I) and (b) 100 (purple curve) and 200 (magenta curve) cycles between 0.05 and 1.6 V vs RHE at 50 mV s^{-1} in O_2-saturated 0.1 M $HClO_4$ (test II). The inset shows the kinetic current density at 0.9 V of Pt_5Gd: sputter cleaned (red), after test I (orange), and after 100 (purple) and 200 (magenta) cycles of test II. For comparison, the kinetic current density of Pt is represented in black.

cycles. Presumably, this loss in activity can be explained by residual contamination from the electrolyte. The CV in N_2-saturated 0.1 M $HClO_4$ taken immediately before the ORR measurements was completely recovered after stability test I (not shown). This <15% deactivation seems to be related to a slight decrease in Gd from the near-surface region: the Pt:Gd XPS ratio at 21° to the sample normal increased from 9.1 (after ORR) to 12.3 (after stability test I, see Figure S5).

Following stability test I, we exposed it to a more aggressive experiment, by cycling it between 0.05 and 1.6 V (i.e., very strong corrosive conditions) at 50 mV s^{-1} in O_2-saturated solutions (test II). After 10 cycles, we did not observe any additional loss in activity in the ORR. However, after 50 cycles between 0.05 and 1.6 V the ORR polarization curve (after stability test I) could not be recovered. As shown in Figure 3b, the sample retains 59% of its initial activity after 100 cycles and 48% after 200 cycles (after ca. 30 h of experiments). Despite these very promising results, the stability of the catalyst will ultimately need to be tested in nanoparticulate form in a PEMFC.

In summary, we present a novel highly active and stable electrocatalyst for the ORR. The activity of Pt_5Gd is similar to that obtained on Pt_3Y in previous studies, which was identified as the most active Pt-based polycrystalline alloy for the ORR.

dx.doi.org/10.1021/ja306348d | J. Am. Chem. Soc. 2012, 134, 16476−16479

Moreover, polycrystalline Pt_5Gd electrodes are extremely stable, resistant to cycling to potentials as positive as 1.6 V. For all these reasons, we expect that alloying Pt with Gd and other rare earths will be a fruitful strategy toward the development of highly active and durable cathodes for PEMFCs.

■ ASSOCIATED CONTENT

Supporting Information

Experimental procedures, computational details, and additional figures. This material is available free of charge via the Internet at http://pubs.acs.org.

■ AUTHOR INFORMATION

Corresponding Author

ibchork@fysik.dtu.dk

Notes

The authors declare no competing financial interests.

■ ACKNOWLEDGMENTS

Financial support is gratefully acknowledged from Energinet.dk through the R&D program ForskEL (CATBOOSTER project) and the Danish Ministry of Science through the UNIK program: Catalysis for Sustainable Energy (CASE). The Center for Individual Nanoparticle Functionality is supported by the Danish National Research Foundation. The Center for Atomic-scale Materials Design is supported by the Lundbeck Foundation.

■ REFERENCES

(1) (a) Gasteiger, H. A.; Kocha, S. S.; Sompalli, B.; Wagner, F. T. *Appl. Catal., B* **2005**, *56*, 9. (b) Stephens, I. E.L.; Bondarenko, A. S.; Grønbjerg, U.; Rossmeisl, J.; Chorkendorff, I. *Energy Environ. Sci.* **2012**, *5*, 6744.

(2) (a) Adzic, R. R.; Zhang, J.; Sasaki, K.; Vukmirovic, J. X.; Shao, M.; Wang, J. X.; Nikelar, A. U.; Mavrikakis, M.; Valerio, J. A.; Uribe, F. *Top. Catal.* **2007**, *46*, 249. (b) Bing, Y.; Liu, H.; Zhang, L.; Ghosh., D.; Zhang, J. *Chem. Soc. Rev.* **2010**, *39*, 2184. (c) Wang, C.; van der Vliet, D.; More, K. L.; Zaluzec, N. J.; Peng, S.; Sun, S.; Daimon, H.; Wang, G.; Greeley, J.; Pearson, J.; Paulikas, A. P.; Karapetrov, G.; Strmcnik, D.; Markovic, N. M.; Stamenkovic, V. R. *Nano Lett.* **2011**, *11*, 919. (d) Rabis, A; Rodriguez, P.; Schmidt, T. J. *ACS Catal.* **2012**, *2*, 864.

(3) (a) Stamenkovic, V.; Mun, B. S.; Mayrhofer, K. J. J.; Ross, P. N.; Markovic, N. M.; Rossmeisl, J.; Greeley, J.; Nørskov, J. K. *Angew. Chem., Int. Ed.* **2006**, *45*, 2897. (b) Stamenkovic, V. R.; Mun, B. S.; Mayrhofer, K. J.J.; Ross, P. N.; Markovic, N. M. *J. Am. Chem. Soc.* **2006**, *128*, 8813. (c) Stamenkovic, V. R.; Fowler, B.; Mun, B. S.; Wang, G. F.; Ross, P. N.; Lucas, C. A.; Markovic, N. M. *Science* **2007**, *315*, 493. (d) Stamenkovic, V. R.; Mun, B. S.; Arenz, M.; Mayrhofer, K. J. J.; Lucas, C. A.; Wang, G. F.; Ross, P. N.; Markovic, N. M. *Nat. Mater.* **2007**, *6*, 241.

(4) (a) Greeley, J.; Stephens, I. E.L.; Bondarenko, A. S.; Johansson, T. P.; Hansen, H. A.; Jaramillo, T. F.; Rossmeisl, J.; Chorkendorff, I.; Nørskov, J. K. *Nat. Chem.* **2009**, *1*, 552. (b) Stephens, I. E.L.; Bondarenko, A. S.; Bech, L.; Chorkendorff, I. *ChemCatChem* **2012**, *4*, 341.

(5) (a) Strasser, P.; Koh, S.; Anniyev, T.; Greeley, J.; More, K.; Yu, C.; Liu, Z.; Kaya, S.; Nordlund, D.; Ogasawara, H.; Toney, M. F.; Nilsson, A. *Nat. Chem.* **2010**, *2*, 454. (b) Stephens, I. E.L.; Bondarenko, A. S.; Perez-Alonso, F. J.; Calle-Vallejo, F.; Jepsen, A. K.; Frydendal, R.; Knudsen, B. P.; Rossmeisl, J.; Chorkendorff, I. *J. Am. Chem. Soc.* **2011**, *133*, 5485.

(6) Strmcnik, D.; Escudero-Escribano, M.; Kodama, K.; Stamenkovic, V. R.; Cuesta, A.; Markovic, N. M. *Nat. Chem.* **2010**, *2*, 880.

(7) Nørskov, J. K.; Rossmeisl, J; Logadottir, A.; Lindqvist, L.; Kitchin, J. R.; Bligaard, T.; Jónsson, H. *J. Phys. Chem. B* **2004**, *108*, 17886.

(8) Toda, T.; Igarashi, H.; Uchida, H.; Watanabe, M. *J. Electrochem. Soc.* **1999**, *146*, 3750.

(9) (a) Mayrhofer, K. J. J.; Hartl, K.; Juhart, V.; Arenz, M. *J. Am. Chem. Soc.* **2009**, *131*, 16348. (b) Chen, S.; Gasteiger, H. A.; Hayakawa, K.; Tada, T.; Shao-Horn, Y. *J. Electrochem. Soc.* **2010**, *157*, A82. (c) Xin, H. L. L.; Mundy, J. A.; Liu, Z.; Cabezas, R.; Hovden, R.; Kourkoutis, L. F.; Zhang, J.; Subramanian, N. P.; Makharia, R.; Wagner, F. T.; Muller, D. A. *Nano Lett.* **2012**, *12*, 490.

(10) (a) Johannesson, G. H.; Bligaard, T.; Ruban, A. V.; Skriver, H. L.; Jacobsen, W.; Nørskov, J. K. *Phys. Rev. Lett.* **2002**, *88*, 255506. (b) Bligaard, T.; Johannesson, G. H.; Ruban, A. V.; Skriver, H. L.; Jacobsen, W.; Nørskov, J. K. *Appl. Phys. Lett.* **2003**, *83*, 4527.

(11) Jakob, K. T.; Waseda, Y. *Mater. Trans., JIM* **1990**, *31*, 135.

(12) Vesborg, P. C.K.; Jaramillo, T. F. *RSC Adv.* **2012**, *2*, 7933.

(13) Yoo, S. J.; Hwang, S. J.; Lee, J.-G.; Lee, S.-C.; Lim, T.-H.; Sung, Y.-E.; Wieckowski, A.; Kim, S.-K. *Energy Environ. Sci.* **2012**, *5*, 7521.

(14) Johansson, T. P. Ph.D. Thesis, Technical University of Denmark: Lyngby, Denmark, 2012.

(15) Kitchin, J. R.; Nørskov, J. K.; Barteau, M. A.; Chen, J. G. *J. Chem. Phys.* **2004**, *120*, 10240.

(16) Pourbaix, M. *Atlas of Electrochemical Equilibria in Aqueous Solutions*; National Association of Corrosion Engineers: Houston, TX, 1974.

(17) Yoo, S. J.; Kim, S.-K.; Jeon, T.-Y.; Hwang, S. J.; Lee, J.-G.; Lee, K.-S.; Cho, Y.-H.; Sung, Y.-E.; Lim, T.-H. *J Chem. Commun.* **2011**, *47*, 11414.

(18) Rossmeisl, J.; Karlberg, G. S.; Jaramillo, T. F.; Nørskov, J. K. *Faraday Discuss.* **2008**, *140*, 337.

(19) Yang, R.; Strasser, P.; Toney, M. F. *J. Phys. Chem. C* **2011**, *115*, 9074.